City University of New York (CUNY)
CUNY Academic Works

International Conference on Hydroinformatics

2014

2D Mathematical Modeling For Fluvial Processes Considering The Influence Of Vegetation And Bank Erosion

Yi Xiao

S.Y. Yang

J. Hu

W.J. Li

S.C. Tong

See next page for additional authors

How does access to this work benefit you? Let us know!

More information about this work at: https://academicworks.cuny.edu/cc_conf_hic/459
Discover additional works at: https://academicworks.cuny.edu

This work is made publicly available by the City University of New York (CUNY).
Contact: AcademicWorks@cuny.edu

Authors
Yi Xiao, S.Y. Yang, J. Hu, W.J. Li, S.C. Tong, and X. H. Fu

This presentation is available at CUNY Academic Works: https://academicworks.cuny.edu/cc_conf_hic/459

2D MATHMATICAL MODELING FOR FLUVIAL PROCESSES CONSIDERING THE INFLUENCE OF VEGETATION AND BANK EROSION

Y.XIAO, S.Y.YANG, J.HU, W.J.LI, S.C.TONG, X.U.FU,Y.CHEN

National Inland Waterway Regulation Engineering Research Center Chongqing Jiaotong University, China

Abstract: A 2D mathematical model for fluvial processes capable of considering the influence of vegetation and non-cohesive bank erosion is established based on a body-fitted coordinate system in this paper. The authors have improved a previously developed simulation model by taking into account the impact of vegetation with a vegetation stress term in the momentum conservation equation. A simple simulation method is adopted in the bank erosion model. Simulation runs were performed for a conceptual alluvial channel, the results of channel plan-form and cross section changes suggest that the 2D model predictions agree acceptable with the classic theories of channel pattern formation considering the effect of vegetation.

Key words: Fluvial process; Influence of vegetation; Vegetation stress term; Non-cohesive bank erosion; 2D numerical model

1. INTRODUTION

Investigating the complex mechanism of patterning processes with various control factors has intrigued geomorphologists and river engineers for several decades. With the rapid developments in numerical methods for fluid mechanics, an advantage of the numerical models is that they can be adapted to test various scenarios which are difficult to test in a physical model, and another advantage is that the cost can be reduced and more options considered. Two- and Three -dimensional computational models have become increasingly popular because of its capabilities in the detail simulations in the flow field, sediment transport and bed topography change in time and space (Nicholas and Smith, 1999; Duan, 2005; Olsen, 2003; XIAO et al.,2010; Filip and Maarten, 2011).

Alluvial channels, adjust themselves to reach regimen conditions not only through the degradation and aggradation of the river bed, but also through width adjustment and planform evolution. The interrelationships between the erodibility of the river banks and the erosive power of the water decide essentially the general direction of channel pattern formation (Chien Ning, 1984). The erodibility of the river banks is not only determined by the bed materials, but also related to the vegetation, which plays a significant role in the channel evolution. Li (1963) increased the roughness of the river bed to reflect the effect of vegetation ignoring the interrelationship between the flow shear stress and bed materials; Shields and Cooper (1998) pointed out that the stability of the river bank is related to vegetation with its influence on the ecological environment for rivers. At present, several studies have been carried out to propose formulations to consider the vegetation effects (Hickin, 1984; Thorne, 1990; Millar, 2000; Bennett et al., 2002). In the numerical models, the relationship between vegetation and stability of the bank can be described by modifying the sediment transport equation (Abt, 1994; Lopez

and Garcia，1998) or flow momentum equation (Pasche and Rouve, 1986; Ikeda and Izumi, 1990).

The objective of this study is to establish a 2D mathematical model for fluvial processes considering the influence of vegetation and non-cohesive bank erosion. In the orthogonal curvilinear coordinates system, the authors improved a previously developed simulation model by taking into account the impact of vegetation with a vegetation stress term in the momentum conservation equation of flow. A simple simulation method was adopted in the non-cohesive bank erosion submodel, which included the influence of river bends, so that it is capable to simulate the formation of sand bars. Simulation runs were performed for a conceptual alluvial channel to investigate the influence of bank vegetation on the channel morphology.

2. HYDRODYNAMIC MODELS CONSIDERING THE INFLUENCE OF VEGETATION

2.1 Governing equations in the Cartesian coordinate system

Governing equations for flow in the Cartesian coordinate system are written as:

$$\frac{\partial}{\partial t}(\rho u_i)+\frac{\partial}{\partial x_j}(\rho u_i u_j)=\rho f_i-\frac{\partial p}{\partial x_i}+\frac{\partial}{\partial x_j}(\tau_{ij}^L-\rho\overline{u_i'u_j'}) \tag{1}$$

The shear-stress tensor term in Eq. (1) can be rewritten as follows：

$$\tau_{ij}=\tau_{ij}^L+\tau_{ij}^T \tag{2}$$

Eq. (1) can be expressed as:

$$\frac{\partial}{\partial t}(\rho u_i)+\frac{\partial}{\partial x_j}(\rho u_i u_j)=\rho f_i-\frac{\partial p}{\partial x_i}+\frac{\partial \tau_{ij}}{\partial x_j} \tag{3}$$

According to previous work by Syunsuke Ikeda (1990), the equilibrium equation for the riparian vegetation zones can be introduced in the form:

$$\frac{\tau}{\cos\theta}=\rho gHS-D_r+\frac{d}{dy}\int_0^H\left(-\rho\overline{u'v'}\right)dz \tag{4}$$

here τ is the total shear stress near the river bank;D_{r} is vegetation stress term; v',u' is fluctuating velocity in the longitudinal and transverse direction, respectively; S is the slope，H is the averaged depth, θ is the angle of the point, often $\theta\approx 0$， Eq.(4) can be rewritten as:

$$\begin{aligned}\tau&=\rho gHS-D_r+\frac{d}{dy}\int_0^H\left(-\rho\overline{u'v'}\right)dz\\ D_r&=\frac{1}{2}\rho C_D\bar{u}^2\frac{aH}{\cos\theta}\\ \tau&=\tau_j^L+\tau^T-D_r\end{aligned} \tag{5}$$

Let $p^v=D_r$， Substitute it to Eq.(1) ,we obtain:

$$\frac{\partial}{\partial t}(\rho u_i)+\frac{\partial}{\partial x_j}(\rho u_i u_j)=\rho f_i-\frac{\partial p}{\partial x_i}+\frac{\partial \tau_{ij}}{\partial x_j}-\frac{\partial p^v}{\partial x_i} \tag{6}$$

here p^v should satisfy the additional condition in all directions as:

$$p^v=\sum_{i=1}^{2}\left(\frac{\partial p^v}{\partial x_i}\right)^2 \tag{7}$$

Substitute Eq.(7) to the governing equations in all directions, we have:

$$\frac{\partial p^v}{\partial x_i}=\frac{\partial\left(\frac{1}{2}\rho C_D\bar{u}^2\frac{aH}{\cos\theta}\right)}{\partial x_i}=\frac{1}{2}\rho C_D\frac{aH}{\cos\theta}\bar{u}u_i \qquad i=1,2 \tag{8}$$

$$\bar{u}=\sqrt{\sum_i u_i^2} \qquad i=1,2 \tag{9}$$

where u is the depth-averaged flow velocity; u_i is the depth averaged flow velocity in the i-direction; a is the vegetation density, defined as $a=d/\ l_x \cdot l_y$; d is the radius of the vegetation; l_x,l_y is the distance of vegetation in the longitudinal and transverse directions.

C_D is the drag coefficient of vegetation. Consider the influence range of the vegetation coefficient, let C_D=1.5 when the vegetation zones near the river bank (Ikeda, 1990); if the zones of vegetation are in the river channel, we assume the influence of vegetation is proportionate to the distance from the channel center in the form:

$$\begin{aligned} C_D &= 0 && x = l \\ C_D &= 1.5 - 1.5x/l && 0 < x < l \\ C_D &= 1.5 && x = 0 \end{aligned} \tag{10}$$

where l is the distance from the river bank to the channel center; x is the distance from the computed point to the river bank.

Substitute Eqs. (8) ~ (9) to the momentum conservation equation of water flow in the Cartesian coordinate system as follows:

$$\begin{aligned} &\frac{\partial(uH)}{\partial t} + \beta\left[\frac{\partial(uuH)}{\partial x} + \frac{\partial(uvH)}{\partial y}\right] - fvH - \frac{1}{2}C_D\frac{aH}{\cos\theta}\sqrt{u^2+v^2}u \\ &+ gH\frac{\partial Z}{\partial x} + \frac{gu|\bar{u}|}{C^2} = \nu_e H\left(\frac{\partial^2 u}{\partial x^2} + \frac{\partial^2 u}{\partial y^2}\right) \\ &\frac{\partial(vH)}{\partial t} + \beta\left[\frac{\partial(uvH)}{\partial x} + \frac{\partial(vvH)}{\partial y}\right] + fuH - \frac{1}{2}C_D\frac{aH}{\cos\theta}\sqrt{u^2+v^2}v \\ &+ gH\frac{\partial Z}{\partial y} + \frac{gv|\bar{u}|}{C^2} - = \nu_e H\left(\frac{\partial^2 v}{\partial x^2} + \frac{\partial^2 v}{\partial y^2}\right) \end{aligned} \tag{11}$$

2.2 Governing equations considering the vegetation effects in the orthogonal curvilinear coordinates system

Based on the advantage of curvilinear coordinates system in simulating the complex topography and stability in computation, the vegetation stress terms are transformed from the Cartesian coordinate system to the orthogonal curvilinear coordinates system as:

$$\begin{aligned} \frac{\partial p^v}{\partial \zeta} &= \frac{1}{2}\rho C_D\frac{aH}{\cos\theta}\sqrt{U^2+V^2}\,\frac{y_\eta h_1 U - y_\xi h_2 V}{J} \\ \frac{\partial p^v}{\partial \eta} &= \frac{1}{2}\rho C_D\frac{aH}{\cos\theta}\sqrt{U^2+V^2}\,\frac{x_\xi h_2 V - x_\eta h_1 U}{J} \end{aligned} \tag{12}$$

Substitute Eq. (12) to the governing equations for water flow in the orthogonal curvilinear coordinates system:

$$\begin{aligned} &\frac{\partial q}{\partial t} + \beta\left(\frac{1}{J}\frac{\partial(h_2 qU)}{\partial \xi} + \frac{1}{J}\frac{\partial(h_1 pU)}{\partial \eta} - \frac{pV}{J}\frac{\partial h_2}{\partial \xi} + \frac{qV}{J}\frac{\partial h_1}{\partial \eta}\right) - fp + \frac{gH}{h_1}\frac{\partial Z}{\partial \xi} + \frac{qg|\bar{q}|}{(CH)^2} \\ &= \frac{\nu_e H}{h_1}\frac{\partial E}{\partial \xi} - \frac{\nu_e H}{h_2}\frac{\partial F}{\partial \eta} + \frac{1}{J}\frac{\partial(h_2 D_{11})}{\partial \xi} + \frac{1}{J}\frac{\partial(h_1 D_{12})}{\partial \eta} + \frac{1}{J}\frac{\partial h_1}{\partial \eta}D_{12} - \frac{1}{J}\frac{\partial h_2}{\partial \xi}D_{22} - \frac{1}{2}\rho C_D\frac{aH}{\cos\theta}\sqrt{U^2+V^2}\,\frac{y_\eta h_1 U - y_\xi h_2 V}{J} \\ &\frac{\partial p}{\partial t} + \beta\left(\frac{1}{J}\frac{\partial(h_2 qV)}{\partial \xi} + \frac{1}{J}\frac{\partial(h_1 pV)}{\partial \eta} + \frac{pU}{J}\frac{\partial h_2}{\partial \xi} - \frac{qU}{J}\frac{\partial h_1}{\partial \eta}\right) + fq + \frac{gH}{h_2}\frac{\partial Z}{\partial \eta} + \frac{pg|\bar{q}|}{(CH)^2} \\ &= \frac{\nu_e H}{h_2}\frac{\partial E}{\partial \eta} + \frac{\nu_e H}{h_1}\frac{\partial F}{\partial \xi} + \frac{1}{J}\frac{\partial(h_2 D_{12})}{\partial \xi} + \frac{1}{J}\frac{\partial(h_1 D_{22})}{\partial \eta} - \frac{1}{J}\frac{\partial h_1}{\partial \eta}D_{11} + \frac{1}{J}\frac{\partial h_2}{\partial \xi}D_{12} - \frac{1}{2}\rho C_D\frac{aH}{\cos\theta}\sqrt{U^2+V^2}\,\frac{x_\xi h_2 V - x_\eta h_1 U}{J} \end{aligned} \tag{13}$$

where h_1,h_2 are lame coefficients in the ξ,η direction; U,V are depth-averaged velocity components in the ξ,η direction; the unit discharge vector is $\bar{q} = (q, p) = (UH, VH)$; Z is water level relative to the reference plane; H is total depth; β is correction factor for non-uniformity of the vertical velocity profile; f is Coriolis parameter; g is gravitational acceleration; C is Chezy coefficient; ν_e is depth mean effective vortex viscosity; z_s、z_b is dependant water level at the water surface and channel bed, respectively.

3. SEDIMENT TRANSPOR MODEL

The sediment transport model can be seen in XIAO et al. (2012).

4. NNUMERICAL ALGORITHM OF NON-COHESIVE BANK EROSION

The influence of bank geometry and river bend is recommended to be considered in the non-cohesive bank erosion model in this study. The computational grid remains stationary in calculation, which ensures that the horizontal positions at all computational nodes remain unchanged, but allows the bed elevation and wet type to be changed. The advantage compared to other models is that in case of a widening or narrowing, the cells keep their dimensions in the plan view and will not be distorted. A memory group is established to handle alterations of dry and wet nodes by storing the information of bank failure.

We adopt an intermittent bank erosion model proposed by Hasegawa (1981). Hasegawa carried out experiments on the process of bank erosion, and found that the bank profiles are similar after bank collapse, forming slopes with the repose angle of sediment. The simplified model of the process of non-cohesive bank erosion is shown in Fig. 1. Line (1) is the initial shape of the side bank, and the side bank profile changes to line (2) after bed scouring. Line (3) shows the bank profile after the upper part of bank (A) collapses and deposits on the bed. The slope angles of lines (1) and (3) β_k are regarded as the angle of repose for the bank materials.

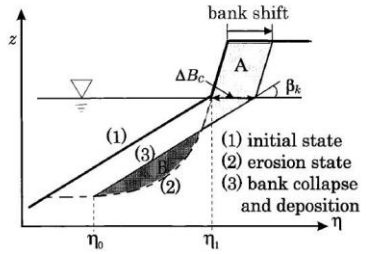

Figure 1 The model of bank failure by Hasegawa (1981)

4.1 Considering the influence of bank geometry for meander bends

Bank erosion processes involve the complex interaction of flow field, bank material and bank geometry. The retreat length at bank collapse ΔB_c depends on the bank size, shapes, and materials, and would be determined by the bank stability (e.g., Darby and Thorne, 1996). In order to simplify numerical procedures, we assume that the lateral erosion distance ΔB_c is obtained by the formula (Osman and Thorne, 1988) as:

$$\Delta B_c = C_l \Delta t(\tau - \tau_c) e^{-0.13\tau_c} / \gamma_{bk} \tag{14}$$

Where C_l is erodibility coefficient, related to bank soil properties; Δt(s) is the time increment; τ_c is the critical shear stress for the bank material; γ_{bk} is the specific weight of bank soil; τ is the flow shear stress acting on the banks in the near bank zone; according to the pioneering works on the effect of secondary flow in meander bends, the distribution of bed shear stress agrees with the longitudinal velocity (Varshney, 1975). The bed shear stress is computed by:

$$\tau = (u/V)^2 \tau_0 = \gamma u^2 / C^2 \tag{15}$$

Owing to the influence of longitudinal and transverse bed-slope, the gravity component may results in the distinction for mechanical characteristics between bank and bed material. In practice, the bank always has a slope so that the incipient motion condition would be different from the condition on a horizontal bottom, the critical shear stress can be expressed by van Rijin(1989):

$$\tau_c = k_1 k_2 \tau_* \tag{16}$$

where τ_* is the critical mobility parameter on a horizontal bottom; the coefficient K_1 is defined as:

$$k_1 = \begin{cases} \sin(\varphi+\beta)/\sin\varphi, & \beta \geq 0 \\ \sin(\varphi-\beta)/\sin\varphi, & \beta < 0 \end{cases}$$
$$k_2 = \cos\gamma(1-\tan^2\gamma/\tan\varphi)^{1/2} \tag{17}$$

where β is the longitudinal bed-slope angle; γ is the transversal bed-slop angle; φ is the angle of response. More details on the expressions of K_1 and K_2 can be found in Julien and Anthony (2002).

In the experiment of Hasegawa (1981), ΔB_c is related to the cross sectional mean velocity according to the field data. The formula of ΔB_c herein would lead to an inaccurate result in the river width adjustment simulation.

Based on the common wet type, we add a new group"2" as the land boundary grid cell which has at least one side next to a water boundary grid cell marked"1" (Fig.2), the bottom elevation at center of the cell is higher than the water stage, and is excluded in the computation for flow and sediment transport. We adopt the largest shear stress to determinate the direction of failure block motion. From Fig. 4, it is assumed that only one side of the land boundary grid cell (i, j+1) can fail, therefore shear stress at the two common sides between the three grid cells are compared and whichever has the largest shear stress fails. The grid cell marked "2" should be included in the solution process for water flow and sediment transport after its bank fails and becomes "wet" (Wang Hong et al., 2010).

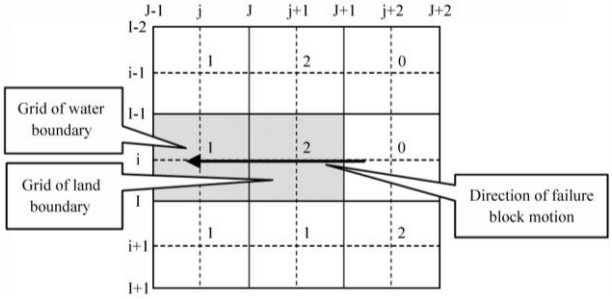

Figure 2 Classification of the bank failure grid

Because the horizontal position of grid points remain unchanged in the computation ,the parameters Δp and ΔL can be used to determine whether the land boundary grid cell should be included in the solution process for water flow and sediment transport after its bank fails and becomes "wet":

$$\Delta p = \frac{h_f}{\tan i_0} \qquad \Delta L = \frac{H}{\tan\beta_k} \tag{18}$$

If $\Delta B + \Delta L > x(i, j+1) - x(i, j)$, as shown in Fig.3a, the land boundary node $(i, j+1)$ should be included in the solution process for water flow and sediment transport, the bed elevation need to be updated as well by the memory group. Reset the memory group after the adjustment of bank failure.

If $\Delta B + \Delta L \leq x(i, j) - x(i-1, j) \leq \Delta B + \Delta L + \Delta p$ (Fig.3b), the bed elevation at land boundary node $(i, j+1)$ is adjusted with geometrical relationship while the wet type remains "2", and the memory group should be involved in the next computational time step with the bank failure information.

If $x(i, j+1) - x(i, j) > \Delta B + \Delta L + \Delta p$ (Fig.3c), both the bed elevation and wet type at land boundary node $(i, j+1)$ are unchanged, and the information of bank failure should be involved in the next time step with the memory group.

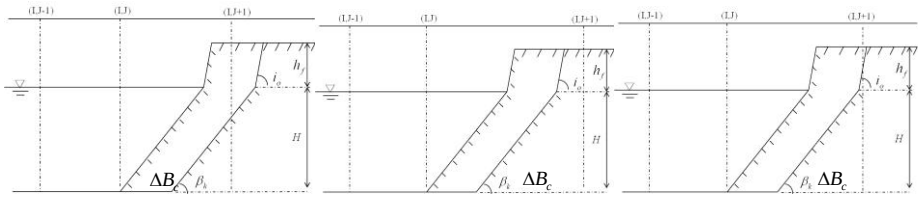

(a) (b) (c)

Figure 3 Calculation methods for bank erosion

5. NUMERICAL EXPERIEMNTS WITH DIFFERENT VEGETATION IMPACTS

The conceptual river is 10000m long and 300m wide shown in Fig.4 (a), the simulation condition is listed in Table1, water level downstream remains constant. A time interval of △ t=6s is applied in the performance during a real time of period of 730 days.

Table 1 The different computed conditions and results

No	Slope ‰	Discharge (m^3/s)	D_{50} （mm）	Time (d)	Bank vegetation Influence
1	0. 4	300-600	1.5	730	No
2	0. 4	300-600	1.5	730	on the downstream bank
3	0. 4	300-600	1.5	730	on the whole river bank

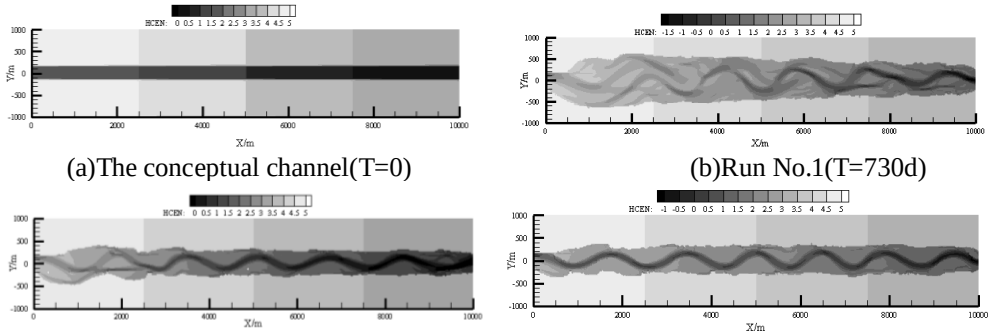

(a)The conceptual channel(T=0) (b)Run No.1(T=730d)

(c)Run No.2(T=730d) (d)Run No.3(T=730d)

Figure 4 Simulated channel patterns after730 days

Figure 4b-d show the final planforms for runs No.1, 2 and 3. It can been seen that a single thread, meandering channel pattern is created in run No. 3, which considered the influence of bank vegetation in the whole river valley. On the other hand, no consideration of bank vegetation lead to a relatively braided river in run No. 1. In run No. 2, we can see the chutes is formed at the apex, a new main channel is produced in the upper part of the river without bank vegetation; the shoal cutting occurred with time processes shown in Fig.5, and a meandering channel is generated in the downstream with the bank vegetation, similar to that in run No.3. Analysis of these results suggests that the bank vegetation contributes to the reinforcement of bank stability: vegetations occupy a large portion of the channel bank strongly affecting the flow distribution, leading to reduction of the shear stress on the bank erosion, and contribute to the formation of meandering channel pattern.

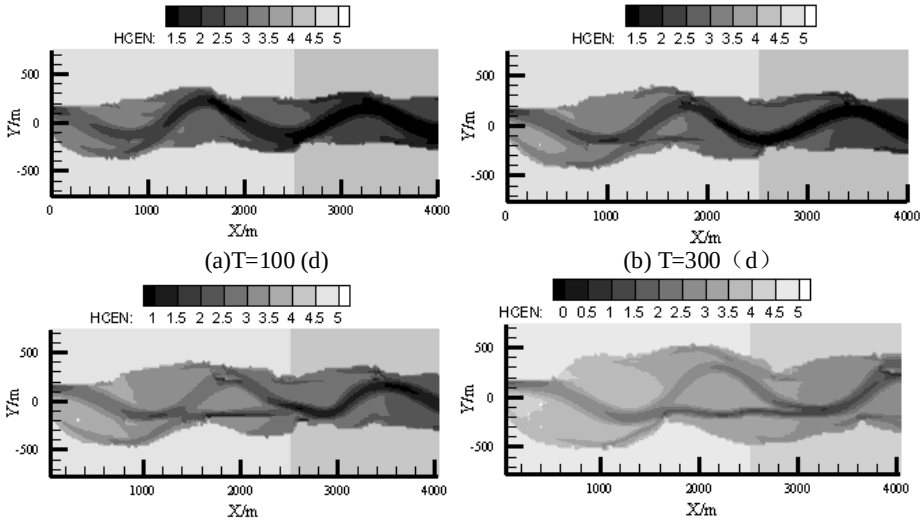

Figure 5 Channel patterns for different time of the upper reach of simulated channel B

Comparison of bed deformations at the 1000m section is shown in Fig.6 for runs No.2~3. A wider, shallower and multi-thread type planform with no vegetation is formed in run No.2 while a narrower and single deep cross section developed with bank vegetation in run No.3. The results implied that the model can reflect the physical mechanics of bank vegetation on channel morphology reasonably: riparian vegetations can be used to increase the streambank stability in river management.

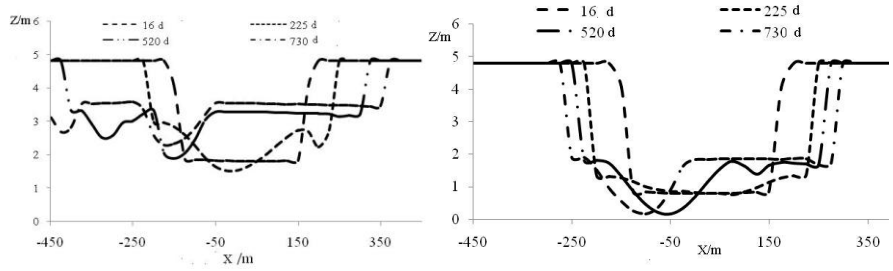

Figure 6 Bed deformation processes at the section of 1000m

6. CONCLSIONS

In this study, impacts of bank vegetation on simulated river patterns agree qualitatively with the existing theories of channel pattern formation machines. However, because of the absence of a theoretical understanding of the interactions of the bank vegetation acting on river planform, further studies are needed to research the physical mechanics to ensure the availability of the numerical model and verify it against field observations or laboratory experiments.

ACKNOWLEDEGEMTNS

This research is supported by the National Key Technology R&D program of china (Grant No. 2012BAB05B00).

REFERENCES

Abt S.R., Clary W.P. and Thornton C.T. Sediment deposition and entrapment in vegetated streambeds. Journal of Irrigation and Drainage Engineering, Vol.120, (1994), p1098.

Bennett,S.J.,Pirim,T. and Barkdoll, B.D. Using simulated emergent vegetation to alter stream flow direction within a straight experimental channel. Geomorphology 44, (2002), pp 115-126.

CHIEN Ning, ZHAN Ren, ZHOU Zhide. Fluvial Processes. Science Press, Beijing, (1987).

Darby, S. E., and Thorne, C. R. Numerical simulation of widening and bed deformation of straight sand-bed rivers. I: Model development. J. Hydr. Engrg., ASCE, 122(4), (1996) , pp 184-193.

Filip SCHUURMAN, Maarten KLEINHANS.Self-formed braided bar pattern in a numerical model. River, Coastal and Estuarine Morphodynamics: RCEM2011, (2011).

Hasegawa, K. Bank-erosion discharge based on a non-equilibrium theory. Proc. JSCE, Tokyo, 316, (1981), pp37-50 (in Japanese).

Hicken, E.J.Vegetation and river channel dynamics. Can.Geographer,(2),(1984),pp111-126.

Ikeda S, Izumi N. Width and depth of self-formed straight gravel rivers with bank vegetation.Water Resources Research, Vol. 26, (1990),pp2353-2364.

Jennifer G. Duan, Pierre Y.Julien. Numerical simulation of the inception of channel meandering.Earth Surface Processes &Landforms, 30(7),(2005),pp1093-1110.

Julien, P.Y., Anthony, D.J. Bed load motion and grain sorting in a meandering stream. J. Hydraul. Res., IAHR 40 (2), (2002), pp125-133.

Kouwen N, Li R.M.Biomechanics of vegetative channel linings. Journal of Hydraulic Engineering, Vol.106, (1980), pp1085-1103.

Lopez F, Garcia M. Open-channel flow through simulated vegetation: Suspended sediment transport modeling. Water Resources Research, Vol.34, (1998), pp2341-2352.

Sheilds Jr. F. D, Cooper C. M. Principles for woody vegetation in river restoration: Problem and Opportunities. Proc. of the International Symposium on River Restoration, Tokyo, Japan, (1998), pp 43-52.

Leo C. van Rijn.Sediment Transport, Part I: Bed Load Transport. Journal of Hydraulic Engineering, ASCE, Vol.110, (1984), pp1431-1456.

LI Baoru.Physical river models. The proceedings of Institute of Water Conservancy and Hydroelectric Power Research, n.10, (1963),pp45-82.

Millar,R.G. Influence of bank vegetation on alluvial channel patterns. Water resources Reasearch, 36(4),(2000), pp1109-1118.

Nicholas AP, Smith GHS. Numerical simulation of three-dimensional flow hydraulics in a braided channel. Hydrologic Processes 13, (1999),pp 913-929.

Osman A M, Thorne C R. Riverbank stability analysis, I: Theory. Journal of Hydraulic Engineering, Vol.114, n.2, (1988), pp134-150.

Olsen N R B. 3D CFD modeling of a self-forming meandering channel.Journal of Hydraulic Engineering, 129(5),(2003), pp366-372.

Pasche E, Rouve M. Over bank flow with vegetative roughened flood plains. Journal of Hydraulic Engineering, ASCE, Vol. 111, n.9,(1986),pp1262-1278.

Thorne,C.R. Effects of vegetation on riverbank erosion and stability in vegetation and erosin,edited by Thornes,J.B.,John Wiley,New York,(1990),pp125-144.

Varshney D V, G arde R J. Shear distribution in bend in rectangular channels. Journal of the Hydraulics Division, ASCE, 101(8), (1975), pp1053-1066.

Van Rijn, L.C. Sediment Transport by Currents and Waves. Report H461,Technical Report, Delft Hydraulics, (1989).

Yi XIAO, Xuejun SHAO, Hong WANG, Gang ZHOU. Formation process of meandering channel by a 2D numerical simulation. International Journal of Sediment Research, 27(3), （2012）, pp306-322.